Liquid Crystals
Publication details, including instructions for authors and subscription information:
http://www.informaworld.com/smpp/title~content=t713926090

Light transmission, linear dichroism and birefringence of nematic/polymer dispersions

O. A. Aphonin; V. F. Nazvanov

Online publication date: 29 June 2010

To cite this Article Aphonin, O. A. and Nazvanov, V. F.(1997) 'Light transmission, linear dichroism and birefringence of nematic/polymer dispersions', Liquid Crystals, 23: 6, 845 — 859
To link to this Article: DOI: 10.1080/026782997207777
URL: http://dx.doi.org/10.1080/026782997207777

LIQUID CRYSTALS, 1997, VOL. 23, NO. 6, 845–859

Light transmission, linear dichroism and birefringence of nematic/polymer dispersions

by O. A. APHONIN*
Advanced Teachers Training Institute, Bol'shaya Gornaya 1, Saratov 410030, Russia

and V. F. NAZVANOV
Department of Physics, University of Saratov, Astrakhanskaya 83, Saratov 410071, Russia

(*Received 24 January 1997; in final form 16 June 1997; accepted 23 July 1997*)

A theoretical study of light transmission, linear dichroism and birefringence of partially ordered dispersions of bipolar nematic droplets in a polymer matrix is presented. The treatment rests on the single scattering approach to an ensemble of uncorrelated and non-interacting anisotropic particles. Theoretical evaluations of the extinction cross sections and phase functions are performed in the anomalous diffraction approximation. Four basic model systems are analysed: PDLC and NCAP films in an external electric field, and PDLC and NCAP films under uniaxial mechanical deformation. The calculated dependences of the generalized parameters characterizing the light transmission, dichroism and birefringence on the angle of incidence of the probing light, droplet size and shape, refractive indices of the LC and polymer, and parameters of the external field are presented graphically and discussed in detail.

1. Introduction

Dispersions of low molecular mass liquid crystals and polymers form a class of composite materials which are currently of high interest because of their importance for both basic research and application [1, 2]. Most commonly, these systems consist of a thin isotropic polymer film containing micron-sized droplets of a nematic liquid crystal (NLC). Optical effects in nematic/polymer dispersions are based on light scattering whose magnitude can be controlled by changing the orientation of the NLC molecules with the help of an external electric or magnetic field, temperature, or directional deformation of the polymer matrix [1, 2].

From the point of view of optics, a nematic droplet in a polymer matrix represents a highly anisotropic birefringent object, in most cases of spherical or elipsoidal shape, in which the local optical axis coincides with the direction of the local NLC director $\hat{\mathbf{n}}(\mathbf{r})$. In the rest state, there is no preferred average direction of $\hat{\mathbf{n}}(\mathbf{r})$ for an ensemble of nematic droplets. This provides an intensive scattering and attenuation of light irrespective of the azimuth of polarization of the incoming beam. Application of an external field or a mechanical deformation of the matrix aligns the liquid crystal molecules inside the droplets so that the whole system behaves as a uniaxial anisotropic medium. This gives rise to considerable changes in the light transmission and, simultaneously, induces two interrelated polarization effects when the direction of incident light does not coincide with the direction of droplet ordering: first is the difference in the extinction of light components polarized parallel and perpendicular to the plane defined by the incoming wave vector and the direction of ordering (*dichroism*) [3–11]; second is the phase shift between these components (*birefringence*) [9–14].

Theoretical analysis of light transmission, linear dichroism and birefringence of nematic/polymer dispersions plays an important role in optimizing projection-type displays for specific applications (the so-called 'direct problem') and, on the other hand, provides diagnostic tools in seeking the structure of this class of anisotropic media ('inverse problem'). Because of the structural complexity of nematic dispersions, an exact theoretical description of propagation of light is not feasible. Approximate models known to date encompass field-controlled light transmission in dispersions formed by phase-separation techniques (PDLC films) [8, 15–18] and by emulsification methods (NCAP films) [19, 20], the field-induced phase shift in PDLC films [13, 14], and the description of dichroism in stretched NCAP

*Author for correspondence.

films [6]. Although these models correctly reflect some experimental situations, they are either restricted by the case of normal incidence of light [15–20], or have a limited range of validity [8, 13, 17, 18].

The aim of this paper is to put the various models together into an explanation of the static electro-optic and mechano-optic response of nematic/polymer dispersions at an arbitrary angle of incidence of the probing light. The treatment rests on the single scattering approach to a system composed of uncorrelated and non-interacting anisotropic particles [10, 11]. Therefore, the exponential (Lambert–Beer) decrease of the transmitted intensity with slab thickness and concentration of scatterers is assumed. These assumptions are reasonable since the directly transmitted light is much less sensitive to co-operative scattering effects than the light scattered out of the incoming beam provided that the collection cone of a detector is sufficiently small [21–24]. The scattering process is analysed in the framework of the anomalous diffraction approximation [3, 10, 25]. We also restrict consideration to a discussion of results obtained for spherical and ellipsoidal NLC droplets with the untwisted bipolar structure [2] which is formed in the case of rigid tangential coupling of NLC molecules with a polymer.

The paper is organized as follows. In § 2, we give the basic background representing the polarization effects in nematic dispersions, not specifying the nature of the orienting field and the form of the orientational distribution function. In § 3 and § 4 this theory is adapted to a description of the static electro-optic and mechano-optic characteristics of nematic/polymer films having the PDLC and NCAP morphology. The main results of the paper are presented in § 5, where we discuss the behaviour of generalized parameters characterizing the light transmission, linear dichroism and birefringence. The conclusions are given in § 6.

2. General formalism

2.1. *Polarization effects in light transmission through a nematic dispersion*

Let us consider a dispersion of nematic droplets embedded in an isotropic polymer medium (matrix), that is placed in an external orienting field **F** of an arbitrary nature. The incident monochromatic beam of wavelength λ is assumed to travel in the direction $\hat{\mathbf{k}}_0$ and makes an angle ϑ_F with the vector **F**. The laboratory Cartesian coordinate system (x, y, z) is chosen so that $\hat{\mathbf{z}} \| \hat{\mathbf{k}}_0$, and the x axis lies in the plane $(\hat{\mathbf{k}}_0, \mathbf{F})$ [figure 1]. All the droplets are assumed to have a cylindrical symmetry of shape and inner structure. Orientation of a droplet is specified by the angular coordinates (ϑ_0, φ_0) or (ϑ, φ) of its symmetry axis $\hat{\mathbf{N}}$ (the droplet director). Polarization of the incident light will be characterized

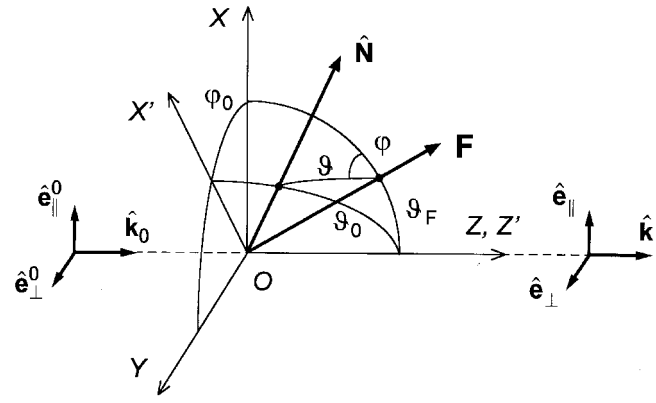

Figure 1. System of coordinates used for description of light transmission in the nematic dispersion. All notations are given in the text.

by two orthogonal vectors $\hat{\mathbf{e}}^0_\parallel$ and $\hat{\mathbf{e}}^0_\perp$ where the indices $\parallel$ and $\perp$ are referred to the plane $(\hat{\mathbf{k}}_0, \mathbf{F})$. The following assumptions are also made: (1) the angular distribution function of the droplet directors, $f(\vartheta, \varphi)$, is symmetric relative to the plane $(\hat{\mathbf{k}}_0, \mathbf{F})$; (2) the dispersion is quite sparse in order to neglect interdroplet correlation effects [22, 26, 27]; (3) the aperture of the detector and the thickness of the slab are sufficiently small to ignore multiple scattering effects [21, 23, 24, 28].

In general, we have to describe the transformation of the Stokes parameters of the incident light in a partially ordered nematic dispersion as a function of the external field **F**. The problem can be solved on examining the propagation of two independent orthogonally polarized waves, $\mathbf{e}_\parallel \| \hat{\mathbf{e}}^0_\parallel$ and $\mathbf{e}_\perp \| \hat{\mathbf{e}}^0_\perp$, which we shall refer to as the normal waves. Using the effective-medium formalism [10, 29, 30], it can be shown that, for the considered combination of symmetries of the nematic droplets and of the whole system, the dilute nematic dispersion is completely characterized by two principal complex refractive indices for the normal waves

$$n_\parallel = n'_\parallel + jn''_\parallel = n_m + 2\pi n_m N k^{-3} \operatorname{Im}\langle A_{xx}\rangle + j2\pi n_m N k^{-3} \operatorname{Re}\langle A_{xx}\rangle, \quad (1a)$$

$$n_\perp = n'_\perp + jn''_\perp = n_m + 2\pi n_m N k^{-3} \operatorname{Im}\langle A_{yy}\rangle + j2\pi n_m N k^{-3} \operatorname{Re}\langle A_{yy}\rangle, \quad (1b)$$

where

$$A_{xx} = A_{11}\cos^2\varphi_0 + A_{22}\sin^2\varphi_0, \qquad A_{yy} = A_{11}\sin^2\varphi_0 + A_{22}\cos^2\varphi_0. \quad (2)$$

Here A_{xx}, A_{yy} are the diagonal elements of the 2×2 forward amplitude scattering matrix of a single droplet, defined in the laboratory frame (x, y, z); A_{11}, A_{22} represent the scattering matrix defined in the coordinate system (x', y', z') related to the droplet [see figure 1; indices

1 and 2 correspond to the light polarization parallel and perpendicular to the plane ($\hat{\mathbf{k}}_0, \hat{\mathbf{N}}$), respectively]; Re and Im stand for the real and imaginary parts; N is the number of droplets per unit volume; $k = 2\pi n_m/\lambda$ is the amplitude of the wave vector in the polymer matrix having the index of refraction n_m; the angle brackets denote a statistical average over parameters characterizing a droplet—orientation, size, shape, etc. With regard to equation (1), the amplitudes and phases of the normal waves are transformed as in a uniaxial crystal:

$$\begin{bmatrix} E_\parallel \\ E_\perp \end{bmatrix} = \begin{bmatrix} \exp\left[-j\frac{2\pi}{\lambda} d(n_\parallel - n_m)\right] & 0 \\ 0 & \exp\left[-j\frac{2\pi}{\lambda} d(n_\perp - n_m)\right] \end{bmatrix} \times \begin{bmatrix} E_\parallel^0 \\ E_\perp^0 \end{bmatrix}, \tag{3}$$

where d is the geometrical path length through the medium. Converting to the Stokes parameters, one can obtain [10, 30]

$$\begin{bmatrix} I_\parallel \\ I_\perp \\ U \\ V \end{bmatrix} = \begin{bmatrix} M_{11} & 0 & 0 & 0 \\ 0 & M_{22} & 0 & 0 \\ 0 & 0 & M_{33} & M_{34} \\ 0 & 0 & -M_{34} & M_{33} \end{bmatrix} \begin{bmatrix} I_{\parallel 0} \\ I_{\perp 0} \\ U_0 \\ V_0 \end{bmatrix} \tag{4}$$

where $(I_{\parallel 0}, I_{\perp 0}, U_0, V_0)$ and $(I_\parallel, I_\perp, U, V)$ are the Stokes vectors for the incident and transmitted light, respectively, and the transformation (Mueller) matrix $\boldsymbol{M}$ contains a total of six non-zero elements, only four of which are essentially different:

$$M_{11} = \exp(-\tau_\parallel d), \qquad M_{22} = \exp(-\tau_\perp d), \tag{5a}$$

$$M_{33} = \cos\psi \exp[-(\tau_\parallel + \tau_\perp)d/2], \quad M_{34} = \sin\psi \exp[-(\tau_\parallel + \tau_\perp)d/2]. \tag{5b}$$

Here

$$\tau_\parallel = N\sigma_\parallel, \qquad \tau_\perp = N\sigma_\perp \tag{6}$$

are the extinction coefficients (also known as the turbidities) for the normal waves, and

$$\psi = \frac{2\pi}{\lambda} d(n'_\parallel - n'_\perp) = Ndg \tag{7}$$

is the phase difference between these waves. The parameters $\sigma_\parallel$, $\sigma_\perp$ are defined as the averaged principal extinction cross sections of a single droplet in the laboratory frame and g is the corresponding elementary phase shift:

$$\sigma_\parallel = 4\pi k^{-2} \mathrm{Re}\langle A_{xx}\rangle = 4\pi k^{-2} \mathrm{Re}\langle A_{11}\cos^2\varphi_0 + A_{22}\sin^2\varphi_0\rangle, \tag{8a}$$

$$\sigma_\perp = 4\pi k^{-2} \mathrm{Re}\langle A_{yy}\rangle = 4\pi k^{-2} \mathrm{Re}\langle A_{11}\sin^2\varphi_0 + A_{22}\cos^2\varphi_0\rangle, \tag{8b}$$

$$g = 2\pi k^{-2} \mathrm{Im}[\langle A_{xx}\rangle - \langle A_{yy}\rangle] = 2\pi k^{-2} \mathrm{Im}\langle (A_{11} - A_{22})\cos(2\varphi_0)\rangle. \tag{8c}$$

Physically, the matrix elements M_{11}, M_{22} are the principal transmission coefficients (transmittances) for the normal waves. The total transmittances for the linearly polarized (L) and unpolarized (U) incident light are given by

$$T_L = M_{11}\cos^2\gamma + M_{22}\sin^2\gamma, \tag{9a}$$

$$T_U = \frac{1}{2}(M_{11} + M_{22}), \tag{9b}$$

where γ stands for the angle between the polarization vector of the incoming light beam and the plane ($\hat{\mathbf{k}}_0, \mathbf{F}$). The difference between M_{11} and M_{22} gives rise to the linear polarization for the originally unpolarized light (*dichroism*); the transmitted light becomes partially linearly polarized either in the plane ($\hat{\mathbf{k}}_0, \mathbf{F}$), if $\tau_\parallel < \tau_\perp$, or perpendicular to this plane, if $\tau_\parallel > \tau_\perp$. The degree of polarization, D, is governed by the parameter of dichroism, $\Delta\tau = \tau_\parallel - \tau_\perp$:

$$D = \frac{M_{22} - M_{11}}{M_{11} + M_{22}} = \frac{\exp(\Delta\tau d) - 1}{\exp(\Delta\tau d) + 1}. \tag{10}$$

The matrix elements M_{33}, M_{34} represent the mutual transformation of linear and circular polarizations due to the phase shift ψ between the normal waves (*birefringence*). At the same time, the equality of other matrix elements to zero excludes the effects of circular dichroism and birefringence [10, 11] from consideration.

For the following discussion, it is useful to express the amplitude scattering matrix elements A_{11} and A_{22} in terms of dimensionless functions:

$$A_{ii} = \frac{k^2}{4\pi}\sigma_g(Q_i + jP_i), \quad i = 1, 2 \tag{11}$$

where σ_g is the geometrical cross section of a droplet in the direction of the incident light, $Q_i = \sigma_i/\sigma_g$ is the conventional extinction efficiency factor [10], and P_i is referred to as the phase function. Using the decomposition (11), the basic optical parameters characterizing the dispersion of bipolar nematic droplets can

be represented as follows

$$\begin{Bmatrix} \tau_{\parallel} \\ \tau_{\perp} \end{Bmatrix} = \frac{C_v}{\langle v_d \rangle} \left\langle \sigma_g \left[\begin{Bmatrix} Q_1 \\ Q_2 \end{Bmatrix} \cos^2 \varphi_0 + \begin{Bmatrix} Q_2 \\ Q_1 \end{Bmatrix} \sin^2 \varphi_0 \right] \right\rangle, \tag{12a}$$

$$\Delta\tau = \tau_{\parallel} - \tau_{\perp} = \frac{C_v}{\langle v_d \rangle} \langle \sigma_g (Q_1 - Q_2) \cos(2\varphi_0) \rangle, \tag{12b}$$

$$\psi = \frac{C_v d}{\langle v_d \rangle} \left\langle \sigma_g \frac{1}{2} (P_1 - P_2) \cos(2\varphi_0) \right\rangle, \tag{12c}$$

where C_v is the volume fraction occupied by droplets, and $\langle v_d \rangle$ is the volume of a droplet averaged over the size distribution.

2.2. *Description of* $\mathbf{Q}_i$ *and* $\mathbf{P}_i$

In the majority of practical cases it is possible to treat Q_i, P_i within the anomalous diffraction approximation (ADA) which deals with optically soft scattering objects larger than the wavelength of light [3, 10, 25]. According to the ADA, the ray picture of light propagation through the droplet is assumed, and the influence of the droplet on the incident plane wave reduces to a distortion of the wave front owing to the different phase shift experienced by different parts of the incident wave; the refraction and reflection at external and internal droplet boundaries are neglected. When the orientation of the local optical axis given by the direction of the local nematic director $\hat{\mathbf{n}}(\mathbf{r})$ varies in space in a complicated manner, only a numerical calculation of Q_i and P_i is possible. Using the anisotropic modification of ADA developed by Zumer and co-workers [3, 25] one can express Q_i and P_i as

$$Q_i = 2\sigma_g^{-1} \int_{\sigma_g} [1 - \mathrm{Re}\{T_{ii}(\mathbf{r}')\}] \, d\sigma_g, \tag{13a}$$

$$P_i = 2\sigma_g^{-1} \int_{\sigma_g} \mathrm{Im}\{T_{ii}(\mathbf{r}')\} \, d\sigma_g, \quad i = 1, 2 \tag{13b}$$

where $T_{ii}(\mathbf{r}')$ are the diagonal elements of the 2×2 transmission matrix for a ray passing through the point specified by the two-dimensional radius-vector $\mathbf{r}'$ at the plane of the amplitude-phase screen approximating the droplet; the screen area coincides with σ_g. The matrix elements $T_{ii}(\mathbf{r}')$ can be worked out with conventional matrix methods. Details of this calculation can be found in the literature [31–33].

An alternative approach for the bipolar droplet uses the concept of an effective index of refraction [8, 13]. The bipolar droplet is assumed to have a uniform uniaxial structure specified by the direction of its symmetry axis $\hat{\mathbf{N}}$. According to the model of Basile *et al.* [13], the corresponding average ordinary and extraordinary indices n_o and n_e can be expressed in terms of the refractive indices of the LC, n_o and n_e, and of the droplet order parameter, $S_d = \frac{1}{2}[3\langle(\hat{\mathbf{N}} \cdot \hat{\mathbf{n}})^2\rangle_{v_d} - 1]$:

$$n_o(S_d) = \frac{2}{\pi} n_o F_m(\pi/2, \tilde{m}), \tag{14a}$$

$$\tilde{m}(S_d) = n_e^{-1} [(2/3)(n_e^2 - n_o^2)(1 - S_d)]^{1/2}, \tag{14b}$$

$$n_e(S_d) = \frac{n_o n_e}{[n_e^2 - (1/3)(n_e^2 - n_o^2)(2S_d + 1)]^{1/2}}, \tag{14c}$$

where $F_m(\pi/2, \tilde{m})$ is the complete elliptic integral of the first kind. In the limit $S_d \to 1$, when $\hat{\mathbf{n}} \| \hat{\mathbf{N}}$ applies everywhere in the droplet, equation (14) gives $n_o(S_d = 1) \equiv n_o$ and $n_e(S_d = 1) \equiv n_e$. For an arbitrary incidence angle ϑ_0, an effective refractive index of the droplet for the component polarized in the plane $(\hat{\mathbf{k}}_0, \hat{\mathbf{N}})$ is given by

$$n_e^{\mathrm{eff}}(\vartheta_0) = \frac{n_o n_e}{(n_e^2 \cos^2 \vartheta_0 + n_o^2 \sin^2 \vartheta_0)^{1/2}}, \tag{15}$$

while the effective index for the orthogonal component does not depend on ϑ_0, being equal to n_o. Such a model allows us to express analytically the elements of the scattering matrix A_{ii} by use of the well-known van de Hulst's formula [10]:

$$A_{ii} = \frac{k^2}{2\pi} \sigma_g \left[1 + \frac{2j}{\rho_i} \exp(j\rho_i) + \frac{2}{\rho_i^2} (1 - \exp(j\rho_i)) \right], \quad i = 1, 2 \tag{16}$$

where

$$\rho_1 = 2ka(\vartheta_0) \left[\frac{n_e^{\mathrm{eff}}(\vartheta_0)}{n_m} - 1 \right], \qquad \rho_2 = 2ka(\vartheta_0) \left[\frac{n_o}{n_m} - 1 \right] \tag{17}$$

are the principal phase shifts along the largest droplet diameter, $2a(\vartheta_0)$, in the direction of the vector $\hat{\mathbf{k}}_0$; the dependence $a(\vartheta_0)$ takes into account the possible non-sphericity of a droplet. From equations (11) and (16), one finds

$$Q_i = 2 - \frac{4}{\rho_i} \sin \rho_i + \frac{4}{\rho_i^2} (1 - \cos \rho_i), \tag{18a}$$

$$P_i = \frac{4}{\rho_i} \cos \rho_i - \frac{4}{\rho_i^2} \sin \rho_i, \qquad i = 1, 2. \tag{18b}$$

In § 5.1 we shall consider the adequacy of this approximate approach in comparison with the more precise equation (13).

2.3. *Averaging procedures*

A statistical average of any orientation-dependent quantity $X(\vartheta_0, \varphi_0)$ in equation (12) can be calculated in

the regular way:

$$\langle X\rangle_{\vartheta\varphi} = \int_0^{2\pi}\int_0^{\pi} X(\vartheta_0, \varphi_0) f(\vartheta, \varphi) \sin\vartheta \, d\vartheta \, d\varphi, \tag{19}$$

where the normalized angular distribution function $f(\vartheta, \varphi)$ describes the probability that the droplet director $\hat{\mathbf{N}}$ lies in the solid angle $\sin\vartheta \, d\vartheta \, d\varphi$, and the angles ϑ_0, φ_0 are related to ϑ, φ by formulae

$$\cos\vartheta_0 = \cos\vartheta\cos\vartheta_F - \sin\vartheta\sin\vartheta_F\cos\varphi, \tag{20a}$$

$$\tan\varphi_0 = \tan\vartheta\sin\varphi/[\sin\vartheta_F + \tan\vartheta\cos\varphi\cos\vartheta_F]. \tag{20b}$$

Averaging over the droplet sizes and shapes is given by

$$\langle X\rangle_a = \int_0^{\infty} X(a)h(a)\,da, \tag{21}$$

where a is either the characteristic droplet size, or the parameter describing its shape (for example, the aspect ratio of an ellipsoid), and $h(a)$ is the corresponding probability density distribution function. To represent $h(a)$, we choose the generalized gamma-distribution [34] which is attractive for modelling all types of nematic dispersions:

$$h(a) = \frac{\eta\, G_1^{\mu+1}}{\Gamma[(\mu+1)/\eta]}\left(\frac{a}{\langle a\rangle}\right)^{\mu}\frac{1}{\langle a\rangle}\exp\left[-G_1^{\eta}\left(\frac{a}{\langle a\rangle}\right)^{\eta}\right], \tag{22a}$$

$$a_m = (\mu/\eta)^{1/\eta} G_1^{-1}\langle a\rangle, \qquad \sigma = G_1^{-1}(G_2 - G_1^2)^{1/2}\langle a\rangle \tag{22b}$$

$$G_1 = \frac{\Gamma[(\mu+2)/\eta]}{\Gamma[(\mu+1)/\eta]}, \qquad G_2 = \frac{\Gamma[(\mu+3)/\eta]}{\Gamma[(\mu+1)/\eta]}. \tag{22c}$$

Here $\Gamma(\ldots)$ is the gamma function; $\langle a\rangle$ and a_m are the average and maximum of the distribution, respectively; σ is the standard deviation; and $\mu > -1$, $\eta > 0$ are the distribution parameters. At $\eta = 1$ expression (22) gives the conventional gamma-distribution.

3. Dispersion of nematic droplets in an external electric field

3.1. PDLC film

For dispersions formed by phase-separation techniques, a conventional structure model assumes that the droplet cavities in the polymer matrix are prolate ellipsoids of revolution ($a, a, b \geq a$), and the symmetry axes of ellipsoids, $\hat{\mathbf{L}}$, are randomly oriented in space with the uniform distribution function $f(\vartheta_L, \varphi_L) = 1/4\pi$ [17, 35]. At zero external field, the director of the bipolar nematic structure in each cavity, $\hat{\mathbf{N}}$, is oriented parallel to the $\hat{\mathbf{L}}$ due to the minimum of the nematic elastic energy in this position that gives $f(\vartheta, \varphi) \equiv f(\vartheta_L, \varphi_L)$. A schematic view of the corresponding thin film geometry is shown in figure 2(*a*). When an external field $\mathbf{E}$ is applied normal to the film plane, the bipolar nematic droplets with positive dielectric anisotropy tend to reorient along the field direction so that the distribution of $\hat{\mathbf{N}}$ becomes axially symmetric. In practice, there is no need to find the corresponding field-dependent function $f(\vartheta, \varphi)$ analytically, since averaging over ϑ can be replaced by averaging over the uniform distribution of ϑ_L if the relationship between the initial, ϑ_L, and current,

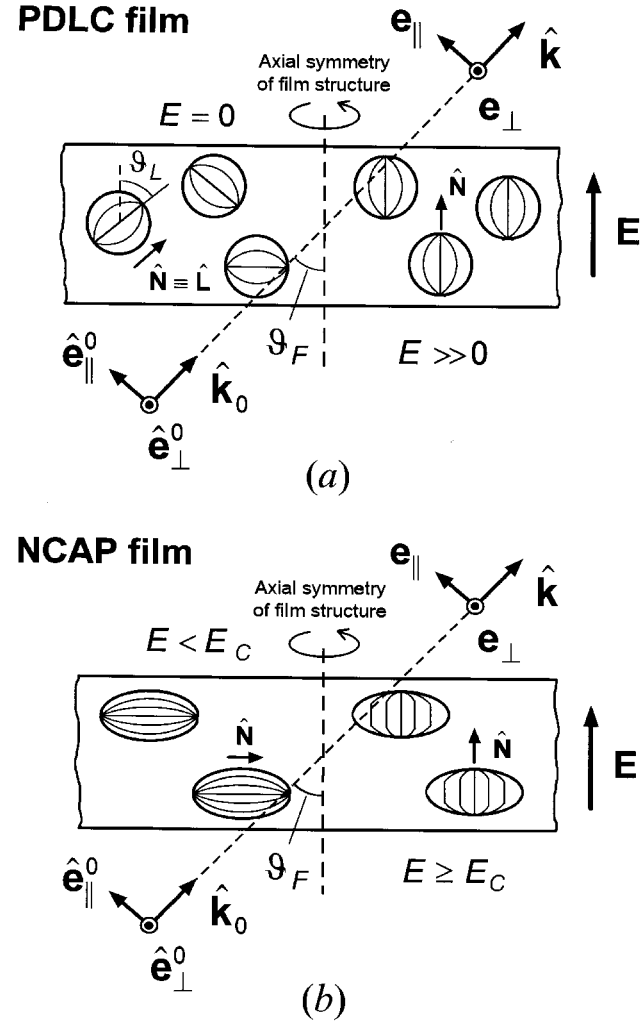

Figure 2. Schematic representation of the orientation of bipolar nematic droplets with respect to the applied field, $\mathbf{E}$, and to the direction of the probing light in PDLC (*a*) and NCAP (*b*) films. Refraction at the film surfaces is not shown; the angle ϑ_F corresponds to the direction of the beam within the film.

$\vartheta(\vartheta_L, E)$, orientation of $\hat{\mathbf{N}}$ is known:

$$\langle X \rangle_{\vartheta\varphi} \equiv \frac{1}{4\pi} \int_0^{2\pi} \int_0^{\pi} X[\vartheta(\vartheta_L, E), \varphi \equiv \varphi_L] \sin \vartheta_L \mathrm{d}\vartheta_L \mathrm{d}\varphi_L, \tag{23}$$

where ϑ, φ are related to ϑ_0, φ_0 by equation (20). According to current models of droplet ordering [17, 35], the equilibrium orientation of $\hat{\mathbf{N}}$ is given by

$$\vartheta = \frac{1}{2} \arctan \left[\frac{\sin(2\vartheta_L)}{e^2 + \cos(2\vartheta_L)} \right], \tag{24}$$

where $e = Ba\xi^{-1}$ is the dimensionless applied field. The parameter B accounts for the droplet shape anisotropy and the surface nematic/polymer interactions [17, 35, 36]; $\xi = E_{\mathrm{in}}^{-1}(K/\Delta\varepsilon)^{1/2}$ is the electric correlation length, where E_{in} stands for the average internal field inside a droplet, K is the NLC elastic constant in the one-constant approximation, and $\Delta\varepsilon$ is the dielectric anisotropy of the liquid crystal. The precise form of B and E_{in} is a subject for discussion that is beyond the scope of this paper. The plot of function $\vartheta(e, \vartheta_L)$ is shown in figure 3. As can be seen, at $\vartheta_L = \pi/2$ the Fréedericksz-type threshold orientational transition $\hat{\mathbf{N}} \perp \mathbf{E} \rightarrow \hat{\mathbf{N}} \| \mathbf{E}$ takes place with the critical field $e_c = 1$.

The optical parameters $\tau_\parallel$, $\tau_\perp$, $\Delta\tau$, ψ can be calculated numerically from equations (12) and (20)–(24) using $\sigma_g = \pi a^2$, $v_d = (4/3)\pi a^3$, and $d = d_0/\cos\vartheta_F$, where a is the radius of a spherical droplet and d_0 is the film thickness along its normal. Since the droplet non-sphericity in a PDLC film is commonly small, say $b/a \leqslant 1{\cdot}2$ [35], the sphere is a good optical model for the droplet shape.

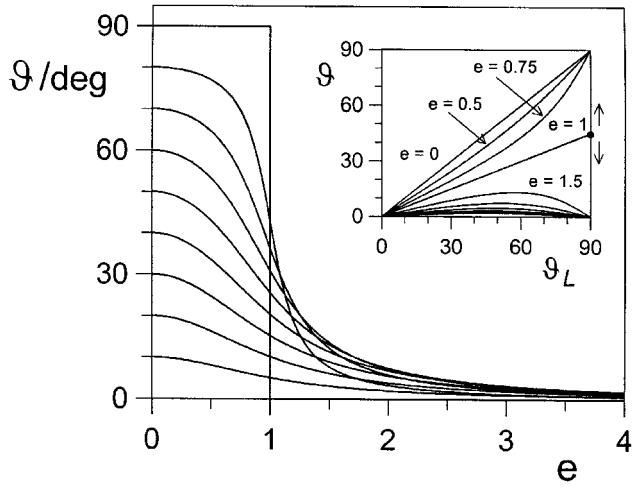

Figure 3. The orientational angle, ϑ, of the bipolar nematic droplet director, $\hat{\mathbf{N}}$, in a PDLC film as a function of the reduced field, e, and of the initial orientational angle, ϑ_L.

3.2. *NCAP film*

In accordance with experimental morphological studies [19, 36, 37], the droplet shape in this case is well approximated by an oblate spheroid ($a, a, b \leqslant a$) having minor axis b oriented along the normal to the film plane. Therefore, at $E = 0$, the droplet directors lie in this plane, but have random azimuthal in-plane orientation; additionally, there is a broad distribution of droplet sizes [19]. A schematic view of the corresponding thin film geometry is shown in figure 2(*b*). The electro-optic response model for the NCAP system can be formulated by considering the distribution of critical switching fields for droplets of different sizes [19, 35, 38]: when $E \geqslant E_c(a_c)$, a particular group of droplets having the size a_c abruptly reorients from the rest state with $\hat{\mathbf{N}} \perp \mathbf{E}$ to the aligned state with $\mathbf{N} \| \mathbf{E}$. Hence one finds

$$\begin{Bmatrix} \tau_\parallel \\ \tau_\perp \end{Bmatrix} = \frac{3C_v l(\vartheta_F)}{4\langle a^3 \rangle} \left\{ \int_0^{a_c^-(E)} a^2 \left\langle \begin{Bmatrix} Q_1(\vartheta_0) \\ Q_2(\vartheta_0) \end{Bmatrix} \cos^2 \varphi_0 + \begin{Bmatrix} Q_2(\vartheta_0) \\ Q_1(\vartheta_0) \end{Bmatrix} \sin^2 \varphi_0 \right\rangle_\varphi h(a)\, \mathrm{d}a + \int_{a_c^+(E)}^{\infty} a^2 \begin{Bmatrix} Q_1(\vartheta_0 = \vartheta_F) \\ Q_2(\vartheta_0 = \vartheta_F) \end{Bmatrix} h(a)\, \mathrm{d}a \right\}, \tag{25a}$$

$$\psi = \frac{3C_v dl(\vartheta_F)}{8\langle a^3 \rangle} \left\{ \int_0^{a_c^-(E)} a^2 \langle [P_1(\vartheta_0) - P_2(\vartheta_0)] \times \cos(2\varphi_0) \rangle_\varphi h(a)\, \mathrm{d}a + \int_{a_c^+(E)}^{\infty} a^2 [P_1(\vartheta_0 = \vartheta_F) - P_2(\vartheta_0 = \vartheta_F)] h(a)\, \mathrm{d}a \right\}, \tag{25b}$$

where $a_c = \xi(E)B^{-1}$ in accordance with equation (24), $l_0 = a/b \approx 1{\cdot}5$ [36, 37] (droplet shape anisotropy is assumed to be independent of droplet size), $l(\vartheta_F) = (l_0^2 \cos^2\vartheta_F + \sin^2\vartheta_F)^{1/2}$, the azimuthal average is given by $\langle X \rangle_\varphi \equiv (1/2\pi)\int_0^{2\pi} X(\vartheta_0, \varphi_0)\, \mathrm{d}\varphi$, and the angles $\vartheta_0, \varphi_0, \vartheta_F, \varphi$ are linked by $\cos\vartheta_0 = -\sin\vartheta_F \cos\varphi$, $\tan\varphi_0 = \tan\varphi/\cos\vartheta_F$. The first integrals in expression (25) represent the droplets maintaining the initial, zero-field orientation, while the second terms describe the droplets oriented along the field.

4. Dispersion of nematic droplets under uniaxial mechanical deformation

There are two basic kinds of mechanical deformation of nematic/polymer films: the shearing of the incompletely polymerized PDLC sample in a preferred direction [35], and the uniaxial stretching of PDLC or NCAP film [5–7, 39]. We shall restrict consideration to

the case of stretching, for it provides the higher degree of droplets ordering.

4.1. *PDLC film*

The undeformed film state is analogous to that described in § 3. The existing theoretical model [6] predicts that, under stretching, each ellipsoidal droplet cavity should be gradually rotated towards the stretch direction **M**, and the droplet director $\hat{\mathbf{N}}$ should be forced to be oriented along $\hat{\mathbf{L}}$ owing to the minimum of the LC elastic energy in this position; simultaneously, the droplets become more elongated. This is illustrated schematically in figure 4 (*a*). Mathematically, the initial ellipsoid of revolution ($a_0, a_0, b_0 > a_0$) having the orientational angle ϑ_{L0} is transformed into the ellipsoid of equal volume with parameters (a, a, b) and ϑ_L given by equations

$$\vartheta_L = \frac{1}{2}\arctan\left(\frac{G}{H_1}\right), \qquad \begin{Bmatrix} a \\ b \end{Bmatrix} = 2^{1/2} a_0 l_0 p [H_2 \pm (G^2 + H_1^2)^{1/2}]^{-1/2}, \tag{26}$$

where

$$G = (l_0^2 - 1) p^{1+\alpha} \sin(2\vartheta_{L0}), \qquad l_0 = b_0/a_0, \tag{27a}$$

$$\begin{Bmatrix} H_1 \\ H_2 \end{Bmatrix} = [l_0^2 p^{2(1+\alpha)} \mp l] \cos^2 \vartheta_{L0} \mp [l_0^2 \mp p^{2(1+\alpha)}] \sin^2 \vartheta_{L0}, \tag{27b}$$

p is the ratio of the film length in the stretched and unstretched states, and $\alpha = 1/2$. The plot of function $\vartheta_L(m, \vartheta_{L0})$ is shown in figure 5 (*a*), where $m = (p-1)/(p_c - 1)$ is the reduced stretch parameter, and $p_c = l_0^{1/(1+\alpha)}$ corresponds to the threshold reorientation $\hat{\mathbf{N}} \perp \mathbf{M} \rightarrow \hat{\mathbf{N}} \| \mathbf{M}$ at $\vartheta_{L0} = \pi/2$ (i.e. when $m = 1$). It is interesting to note the close parallels between the dependence $\vartheta(e, \vartheta_L)$ in figure 3 and the dependence $\vartheta_L(m, \vartheta_{L0})$ in figure 5 (*a*); this allows us to treat m as a measure of the 'mechanical field'. Figure 5 (*b*) illustrates the change in the film order parameter, $S_F = \frac{1}{2}[3\langle\cos^2\vartheta_L\rangle - 1]$, calculated using equations (26) and (27).

The optical response of the film is given by equations (12), (20), (21) and (23) with geometrical parameters $\sigma_g(\vartheta_0) = \pi a (a^2 \cos^2\vartheta_0 + b^2 \sin^2\vartheta_0)^{1/2}$, $v_d = (4/3)\pi a^2 b$.

4.2. *NCAP film*

In this case, the oblate spheroidal droplet cavities ($a_0, a_0, b_0 < a_0$) are transformed to prolate ellipsoids (a, b, c) as shown in figure 4 (*b*). The mechanism of the ordering of the droplet directors $\hat{\mathbf{N}}$ can be more complicated than that described above; the extended discussion of possible experimental situations may be found in reference [39].

In the most interesting case of normal incidence ($\vartheta_F = \vartheta_0 = \pi/2$, $\varphi_0 = \vartheta$), the optical parameters of the film can be expressed as

$$\begin{Bmatrix} \tau_\parallel \\ \tau_\perp \end{Bmatrix} = \frac{3 C_v l_0}{4\langle a_0^3\rangle}\left[\left\langle a_0^2 \begin{Bmatrix} Q_2 \\ Q_1 \end{Bmatrix}\right\rangle_a \pm \frac{1}{2}\langle a_0^2 (Q_1 - Q_2)\rangle_a (1 + S_F)\right], \tag{28a}$$

$$\psi = \frac{3 C_v d_0 l_0}{8\langle a_0^3\rangle}\langle a_0^2 (P_1 - P_2)\rangle_a S_F, \tag{28b}$$

where $S_F = 2\langle\cos^2\vartheta\rangle - 1$ is the two-dimensional film order parameter. The experimentally obtained dependence of S_F [39] on the stretch parameter, $t \equiv p - 1$, is shown in figure 5 (*b*).

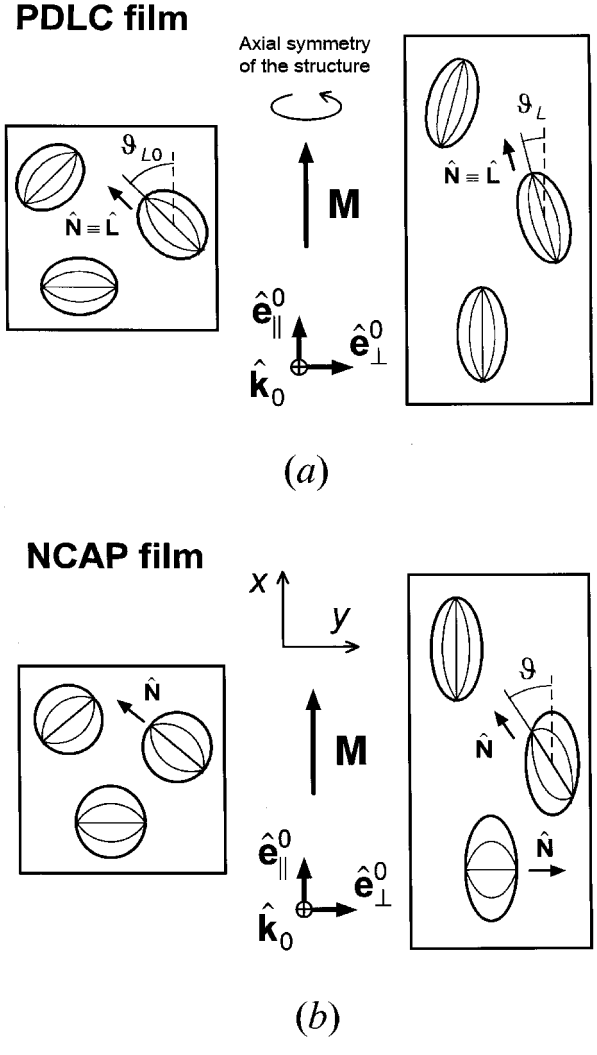

Figure 4. Schematic representation of the orientation of bipolar nematic droplets in uniaxially stretched PDLC (*a*) and NCAP (*b*) films. Unstretched (left) and stretched (right) states are shown.

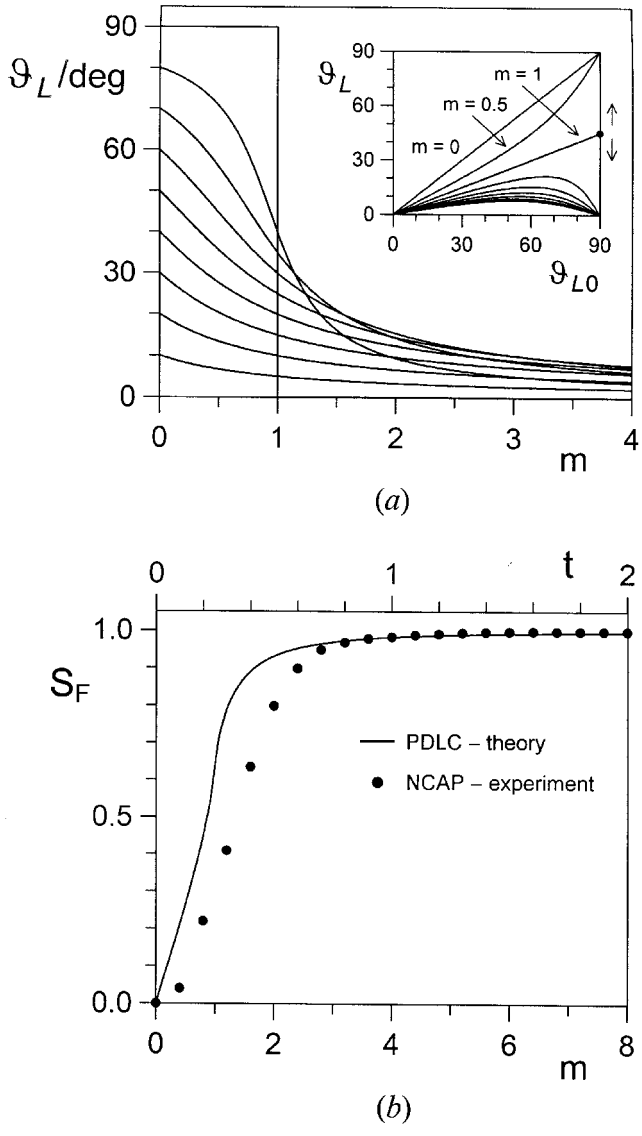

Figure 5. Characteristics of the orientational ordering of bipolar nematic droplets in a stretched PDLC film: (*a*) dependences of the droplet orientational angle, ϑ_L, on the stretch parameter, m, and initial orientational angle, ϑ_{L0}; (*b*) the dependence of the film order parameter, S_F, on m. The dots represent the experimental dependence of S_F on the stretch parameter, t, for the NCAP film [39].

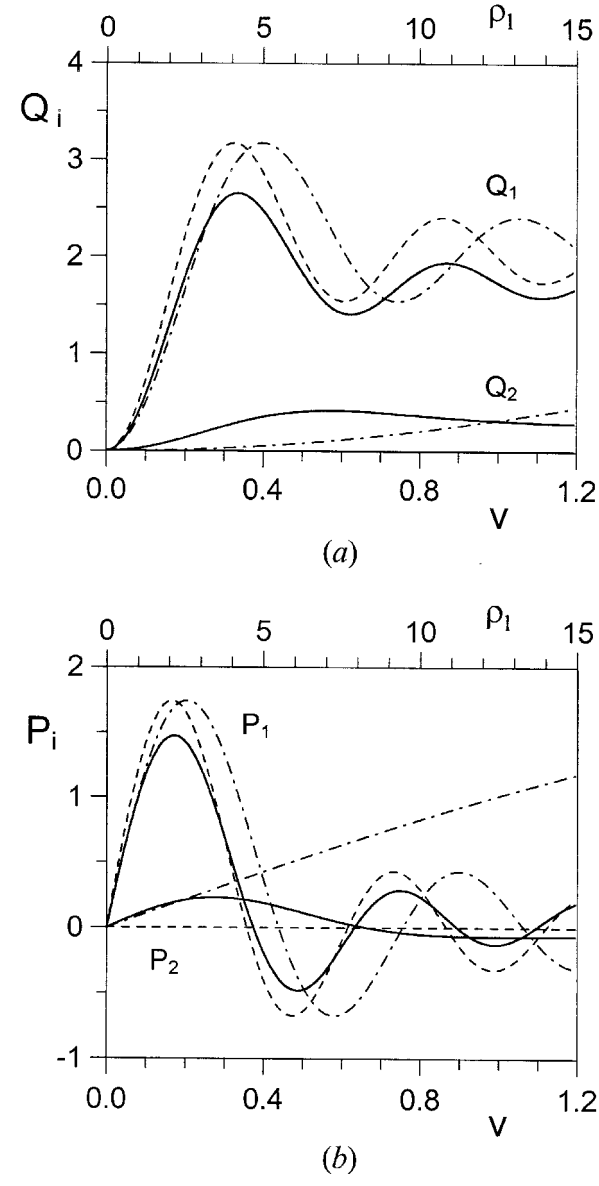

Figure 6. The dependence of the principal extinction efficiency factors, Q_i, and phase functions, P_i, of the spherical bipolar nematic droplet on the phase parameters, v and ρ_1 for the case of index matching, $n_o = n_m$, at $\vartheta_0 = 90°$. The full lines represent the bipolar director configuration [equations (13), (29), (30)], the broken lines correspond to the uniform droplet model [equations (14)–(18) with $S_d = 1$], and the chain lines are used for the Basile approach [equations (14)–(18) with $S_d = 0{\cdot}76$].

5. Numerical results and discussion

5.1. *Extinction efficiency factors and phase functions*

Figure 6 shows the extinction efficiency factors Q_i and phase functions P_i of the spherical bipolar nematic droplet, plotted versus the phase parameters ρ_1 and v for $\vartheta_0 = 90°$ (i.e. $\hat{\mathbf{N}} \perp \hat{\mathbf{k}}$). The parameter $v = a(n_e - n_o)/\lambda$ is directly related to ρ_1 ($\rho_1 = 4\pi v$), but is more descriptive for the analysis of possible experimental situations. The angular dependencies $Q_i(\vartheta_0)$, $P_i(\vartheta_0)$ are presented in figure 7. Calculations were performed numerically, using equation (13), for the practically most important case of index matching, $n_o = n_m$. The bipolar director field was modelled by segments of circles passing through both droplet poles [20, 40]. In cylindrical coordinates $(\tilde{\rho}, \phi, \zeta)$ attached to the droplet symmetry axis $\hat{\mathbf{N}}$ the corresponding director field lines are given by equation (29) [41]

$$\left(\tilde{\rho} - \frac{a}{\tan\tilde{\sigma}}\right)^2 + \zeta^2 = \left(\frac{a}{\sin\tilde{\sigma}}\right)^2, \qquad (29)$$

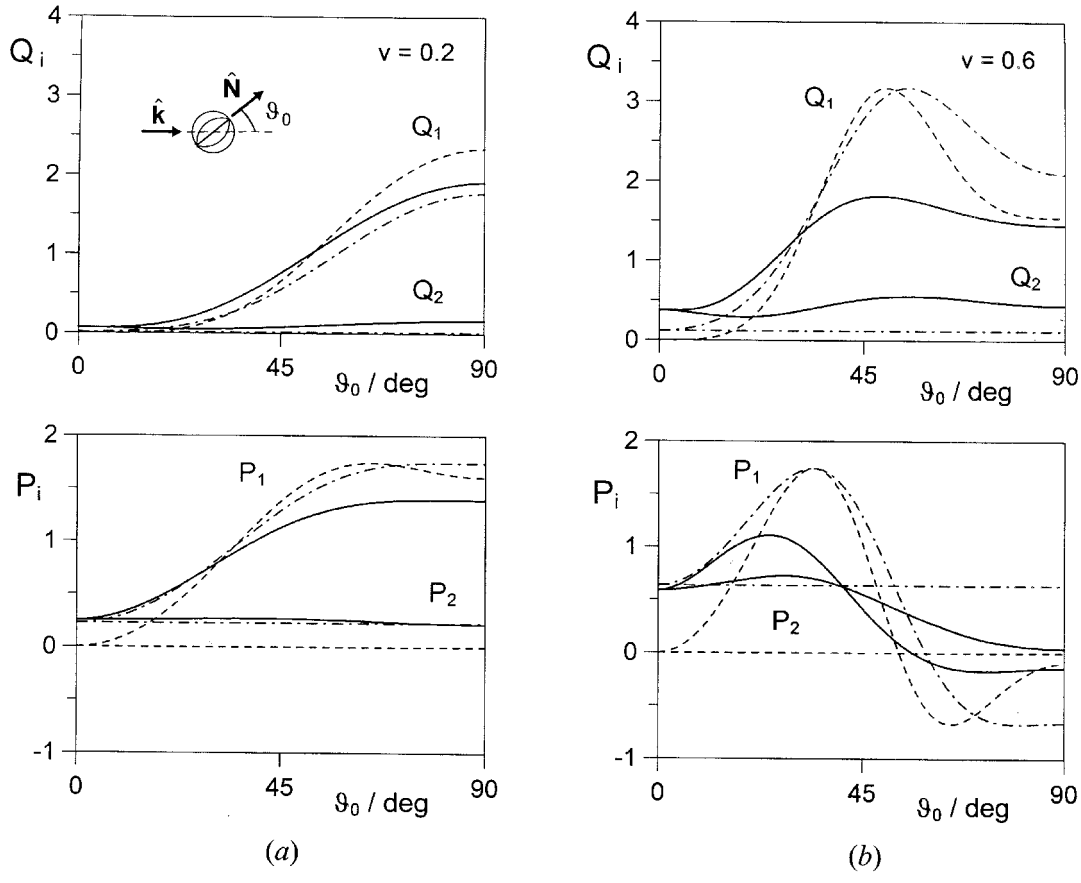

Figure 7. The angular dependence of Q_i and P_i of the spherical bipolar nematic droplet for $v=0{\cdot}2$ (*a*) and $v=0{\cdot}6$ (*b*); $n_o=n_m$. Curves are assigned using the same convention as in figure 6.

where

$$\cos\tilde{\sigma}=\cosh\tilde{\tau}-\frac{a\sinh\tilde{\tau}}{\zeta},\qquad \tilde{\tau}=\frac{1}{2}\ln\frac{\tilde{\rho}^2+(\zeta+a)^2}{\tilde{\rho}^2+(\zeta-a)^2}. \tag{30}$$

Also shown in figures 6 and 7 are the dependencies $Q_i(v)$, $P_i(v)$ calculated using equations (14)–(18) for the droplet having the uniform director configuration (UC), when $\hat{\mathbf{n}}\|\hat{\mathbf{N}}$ and $S_d=1$, and for the droplet with the average indices $n_e(S_d)$, $n_o(S_d)$ corresponding to the bipolar director field ($S_d\approx 0{\cdot}76$). From these data it is possible to examine the range of validity of the UC-model which has intuitively been used in many studies as an approximation for the droplet having a bipolar structure when considering the light extinction and scattering phenomena [3, 13, 15–18, 20, 23, 42–44].

The following observations can be made:

(a) The general behaviour of Q_1 and P_1 for the bipolar droplet is the same as for the droplet with the uniform structure. At small values of v, both Q_1 and P_1 increase monotonically, but then start to oscillate around their asymptotic values due to the constructive and destructive interference between transmitted and diffracted light. The positions of the maxima and minima of $Q_1(v)$ and $P_1(v)$ coincide with those of the uniform droplet, but the magnitudes are lower over the entire range of v. At the same time, Q_2 and P_2 diverge considerably from zero as opposed to the droplet with the uniform structure which has no ordinary ray scattering at $n_0=n_m$. The asymptotic behaviour of $Q_i(v)$ and $P_i(v)$ for the bipolar droplet case is governed by $\lim_{v\to\infty}Q_1<2$, $\lim_{v\to\infty}Q_2>0$, $\lim_{v\to\infty}(Q_1+Q_2)\approx 2$, and $\lim_{v\to\infty}P_1=\lim_{v\to\infty}P_2=0$.

(b) The angular dependencies of Q_i and P_i are well approximated by the UC-model at $v\leqslant 0{\cdot}3$. For larger v, the discrepancy considerably increases, although the van de Hulst formulae (18) still give the right qualitative description of the numerical results up to $v\approx 0{\cdot}4$–$0{\cdot}6$.

(c) The effective refractive index approximation proposed by Basile *et al.* [13] (chain lines in figure 6; $S_d=0{\cdot}76$) works well for Q_1, P_1, and P_2 at $v<0{\cdot}2$–$0{\cdot}3$, but underestimates the numerically calculated Q_2 in this region. At higher v, this approximation does not provide acceptable accuracy.

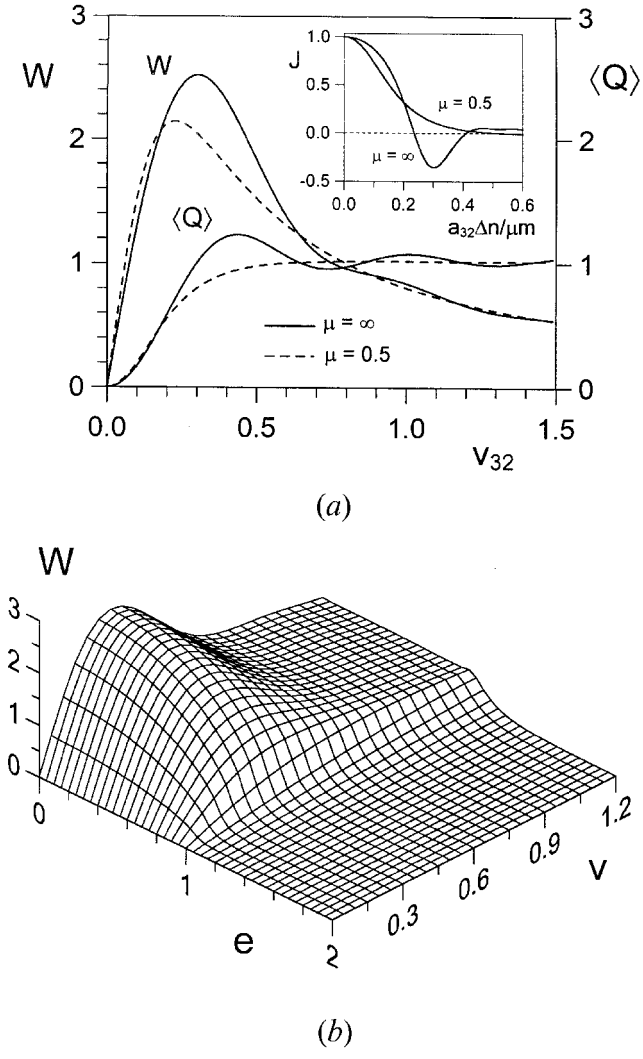

Figure 8. Light transmission characteristics of an electrically controlled PDLC film at normal incidence. (*a*) The reduced turbidity, W, and the average extinction efficiency factor, $\langle Q \rangle$, at zero field as functions of the phase parameter, $v_{32} = a_{32}\Delta n/\lambda$, and the width of droplet size distribution. The gamma-distribution with $\mu \to \infty$ (monodispersion) and $\mu = 0{\cdot}5$ (wide spread of droplet sizes) is used. The inset shows the normalized average steepness, $J = [\tau(\lambda_{min}) - \tau(\lambda_{max})]/\tau(\lambda_{min})$, of the spectral dependence of zero-field turbidity versus the product $a_{32}\Delta n$ ($\lambda_{min} = 400\,nm$, $\lambda_{max} = 700\,nm$, $n_o = n_m$). (*b*) The characteristic surface, $W(e, v)$, for the electro-optic response of the monodisperse PDLC film; all data correspond to the case $n_o = n_m$.

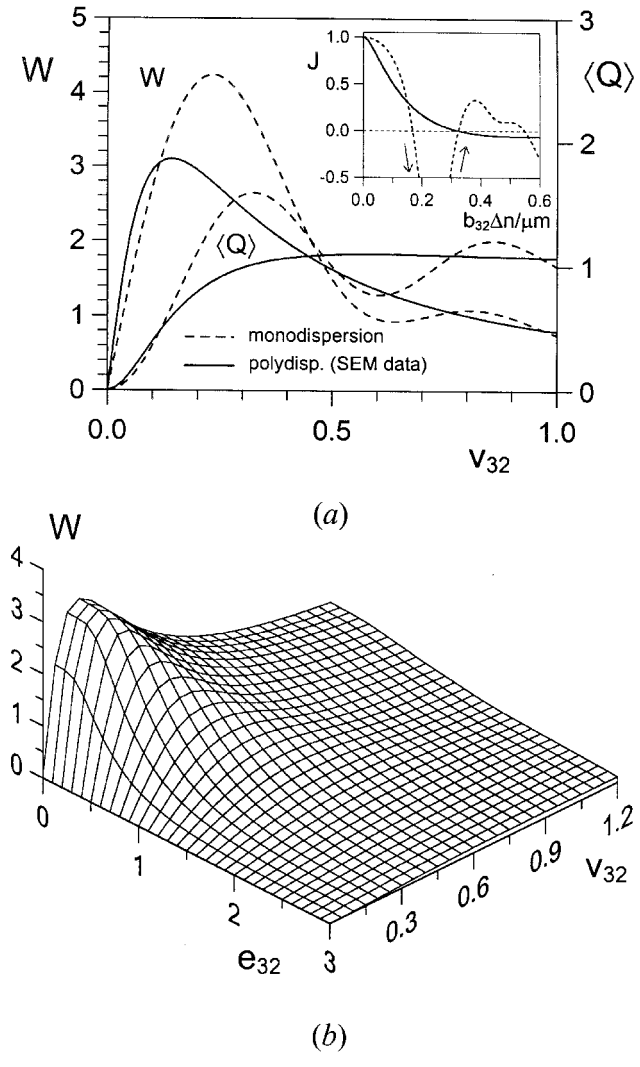

Figure 9. Light transmission characteristics of electrically controlled NCAP film at normal incidence. (*a*) The reduced turbidity, W, and the average extinction efficiency factor, $\langle Q \rangle$, at zero field as functions of the phase parameter, v_{32}. The curve designated as SEM (Scanning Electron Microscopy) corresponds to the droplet size distribution extracted from the experimental data [37] [equation (22) with parameters $\mu = 4$, $\eta = 0{\cdot}26$]. The inset shows the average steepness, J, of the spectral dependence of zero field turbidity as a function of the product $b_{32}\Delta n$. (*b*) The characteristic surface, $W(e_{32}, v_{32})$, for the electro-optic response of the polydisperse (SEM data) NCAP film; all data correspond to the case $n_o = n_m$.

The above analysis permits one to draw the following conclusion: the use of simple anomalous diffraction formulae (18) for modelling Q_i and P_i of the bipolar droplet may be treated as reasonably correct if $v \leqslant 0{\cdot}2$–$0{\cdot}4$; in the region $v > 0{\cdot}4$, only the qualitative description is possible.

This is also valid for the elongated bipolar droplets. The relevant plots can be found in reference [33].

5.2. *Characteristics of electrically controlled PDLC and NCAP films*

5.2.1. *Light transmission at normal incidence*

From the practical standpoint, two questions are important for the optimization of PDLC and NCAP displays working in a transmission mode [1, 2]: how do the geometrical and material parameters of a nematic/polymer dispersion affect its zero-field transmission and,

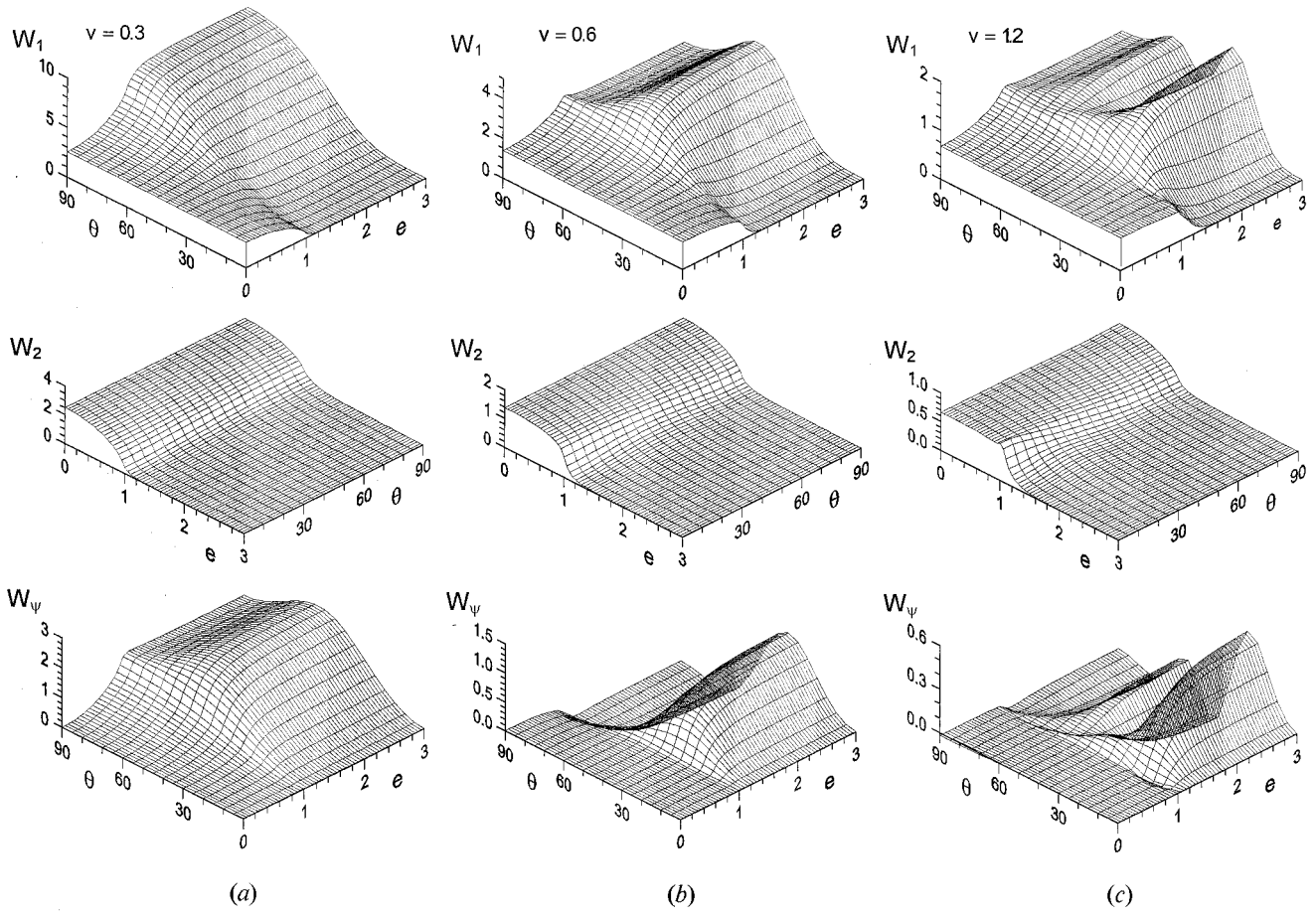

Figure 10. The characteristic surfaces for the angular dependences of the reduced principal turbidities, $W_1(\vartheta_F, e)$, $W_2(\vartheta_F, e)$, and the reduced phase shift, $W_\psi(\vartheta_F, e)$, of electrically controlled monodisperse PDLC. Three typical values of the droplet phase parameter are used: $v = 0{\cdot}3$ (*a*) $0{\cdot}6$ (*b*), $1{\cdot}2$ (*c*); $n_o = n_m$, $\vartheta \equiv \vartheta_F$.

secondly, how do these parameters influence the shape of the transmission curve, $T(e)$?

The effects of the droplet size, LC birefringence, and light wavelength on the zero-field turbidity of PDLC film have been treated both theoretically and experimentally in a number of studies [2, 26, 43–45]. The results obtained have revealed that: (1) there is a maximum in the dependence $\tau(a)$; (2) the amplitude of this maximum is directly proportional to $\Delta n = n_e - n_m$ and is inversely proportional to λ; (3) the position of the maximum is governed by the parameter $v_{max} = a\Delta n/\lambda \approx 0{\cdot}3$.

To generalize these findings, we introduce the dimensionless reduced turbidity, W, which is related to τ by $\tau = (C_V \Delta n/\lambda) W$. As an argument which is best suited to characterize the polydisperse system of droplets, we use the parameter $v_{32} = a_{32}\Delta n/\lambda$, where $a_{32} = \langle a^3 \rangle / \langle a^2 \rangle$. For the simple gamma-distribution, $a_{32} = a_m(\mu + 1)/\mu = \langle a \rangle (\mu + 2)/(\mu + 1)$ and $\lim_{\mu \to \infty} a_{32} = a_m$. The plots of functions $W(v_{32})$ for the PDLC and NCAP films are shown in figures 8(*a*) and 9(*a*), respectively, together with the associated average extinction efficiency factors, $\langle Q(v_{32}) \rangle$.† These plots may be regarded as the *characteristic curves* whereby the zero-field transmission can be optimized.‡

The curve $W(v_{32})$ is convenient for the minimization of $T(e = 0)$ at a given wavelength by adjusting the droplet size and LC birefringence. Depending on the size distribution function, the position of the extremum v_{max} and its magnitude $W(v_{max})$ lie in the ranges

$$v_{max} \approx 0{\cdot}2 \to 0{\cdot}3, \qquad W_{max} \approx 2{\cdot}1 \to 2{\cdot}6 \qquad (31\,a)$$

† Having regard to the discussion in §5.1, the simulations performed in this paragraph and in §5.3 are based on the uniform droplet model for Q_i and P_i.

‡ Strictly speaking, such a presentation does not take into account the wavelength dependence of the refractive indices of the LC and polymer. However, in the visible region $n_{e,o}(\lambda)$ and $n_m(\lambda)$ vary at nearly the same rate [46, 47] giving $n_e - n_m \approx$ const, $n_o - n_m \approx$ const.

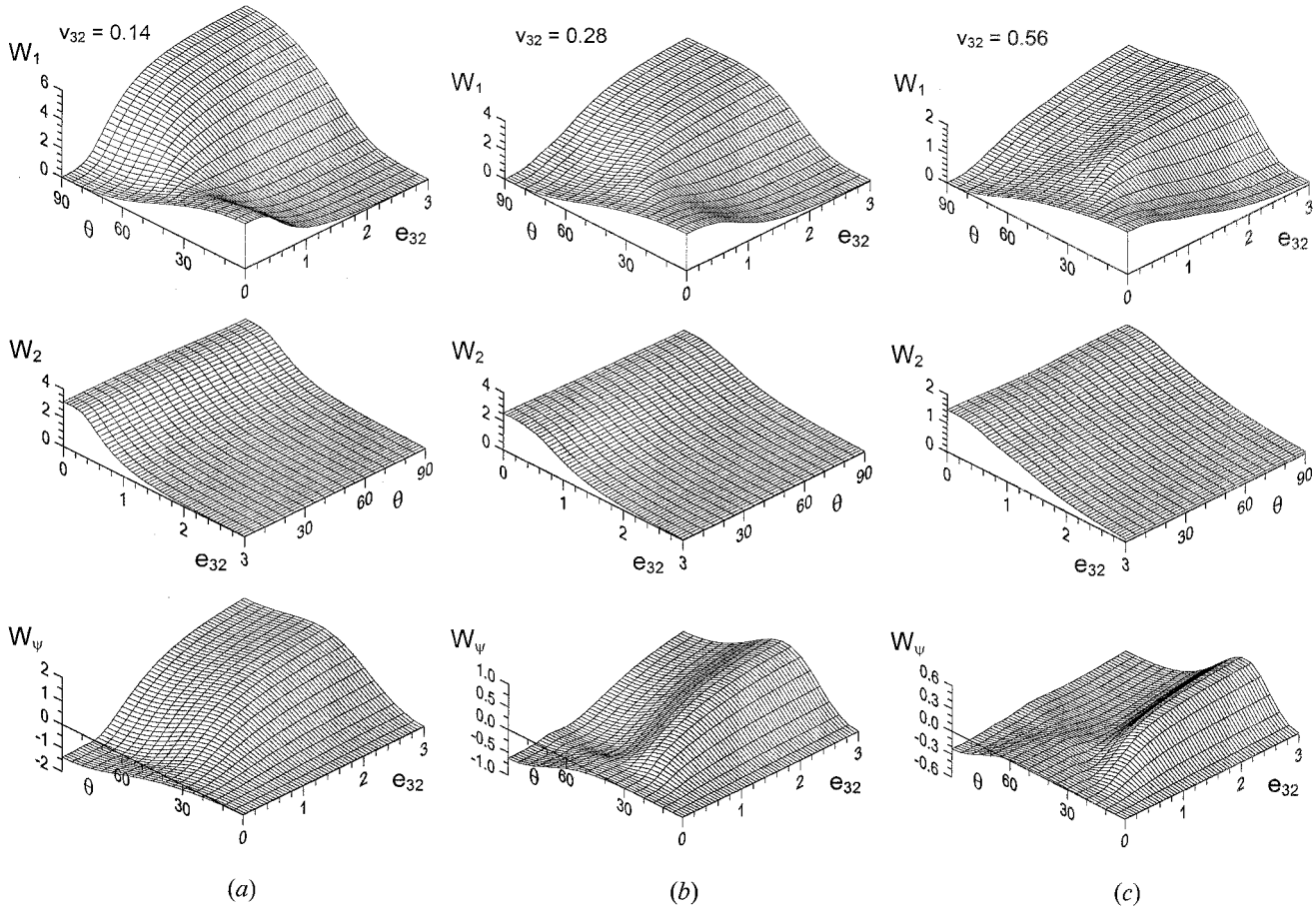

Figure 11. The characteristic surfaces for the angular dependences of the reduced principal turbidities, $W_1(\vartheta_F, e_{32})$, $W_2(\vartheta_F, e_{32})$, and the reduced phase shift, $W_\psi(\vartheta_F, e_{32})$, of electrically controlled polydisperse (SEM data) NCAP film at $v_{32}=0{\cdot}14$ (*a*), $0{\cdot}28$ (*b*), $0{\cdot}56$ (*c*); $n_o=n_m$, $\vartheta\equiv\vartheta_F$.

for the PDLC film and in the ranges

$$v_{max}\approx 0{\cdot}15\rightarrow 0{\cdot}25, \qquad W_{max}\approx 3{\cdot}1\rightarrow 4{\cdot}3 \qquad (31\,b)$$

for the NCAP film.

The spectral behaviour of $T(e=0)$ is governed by the dependence $\langle Q(\lambda)\rangle$. In practice, it is desired to avoid the 'red-bleedthrough' effect when the film is more transparent to the long wavelength part of a given spectral region [15, 43]. As follows from the presented data, the onset for this phenomenon occurs at

$$v_{PDLC}\leqslant 0{\cdot}6, \qquad v_{NCAP}\leqslant 0{\cdot}5. \qquad (32)$$

To obtain a more precise estimation for the visible region, we have calculated the normalized average steepness, $J=[\tau(\lambda_{min})-\tau(\lambda_{max})]/\tau(\lambda_{min})$, of the dependence $\tau(\lambda)$ as a function of $a_{32}\Delta n$; these results are shown in the insets of figures 8(*a*) and 9(*a*) for $\lambda_{min}=400$ nm and $\lambda_{max}=700$ nm. As clearly seen, the monodisperse films are characterized by 'zero-points' $(a\Delta n)_{PDLC}\approx\{0{\cdot}23; 0{\cdot}40\}$ and $(b\Delta n)_{NCAP}\approx\{0{\cdot}17; 0{\cdot}32\}$, while for the polydisperse films the red-bleedthrough onset occurs when $(a_{32}\Delta n)_{PDLC}\leqslant 0{\cdot}45$ and $(b_{32}\Delta n)_{NCAP}\leqslant 0{\cdot}3$. The latter values are consistent with the results of Drzaic [43]; they are also supported by the experimental data extracted from the work of Nomura *et al.* [45].

A further extension of the characteristic curve $W(v_{32})$ is the *characteristic surface*, $W(v_{32}, e_{32})$, which completely represents the electro-optic response of a nematic/polymer dispersion for a given droplet size distribution. By analogy with v_{32}, the reduced field $e_{32}=Ba_{32}\xi^{-1}$ has been found to describe best the polydisperse system of droplets. The relevant three-dimensional plots are shown in figures 8(*b*) and 9(*b*) for the case $n_o=n_m$. The normal transmittance can easily be obtained from these data by the Lambert–Beer law, $T=\exp(-C_V\Delta n\lambda^{-1}Wd_0)$. As can be seen, the parameter v_{32} substantially affects the shape of the $W(e_{32})$ curve. For the PDLC film, $W(e_{32})$ reaches its saturation at higher fields and has a much sharper field threshold when v_{32} increases. This is in agreement with the observation made originally by Kelly *et al.* [15]. Figure 9(*b*) reveals that the first of these tendencies is also valid for the NCAP film, but the

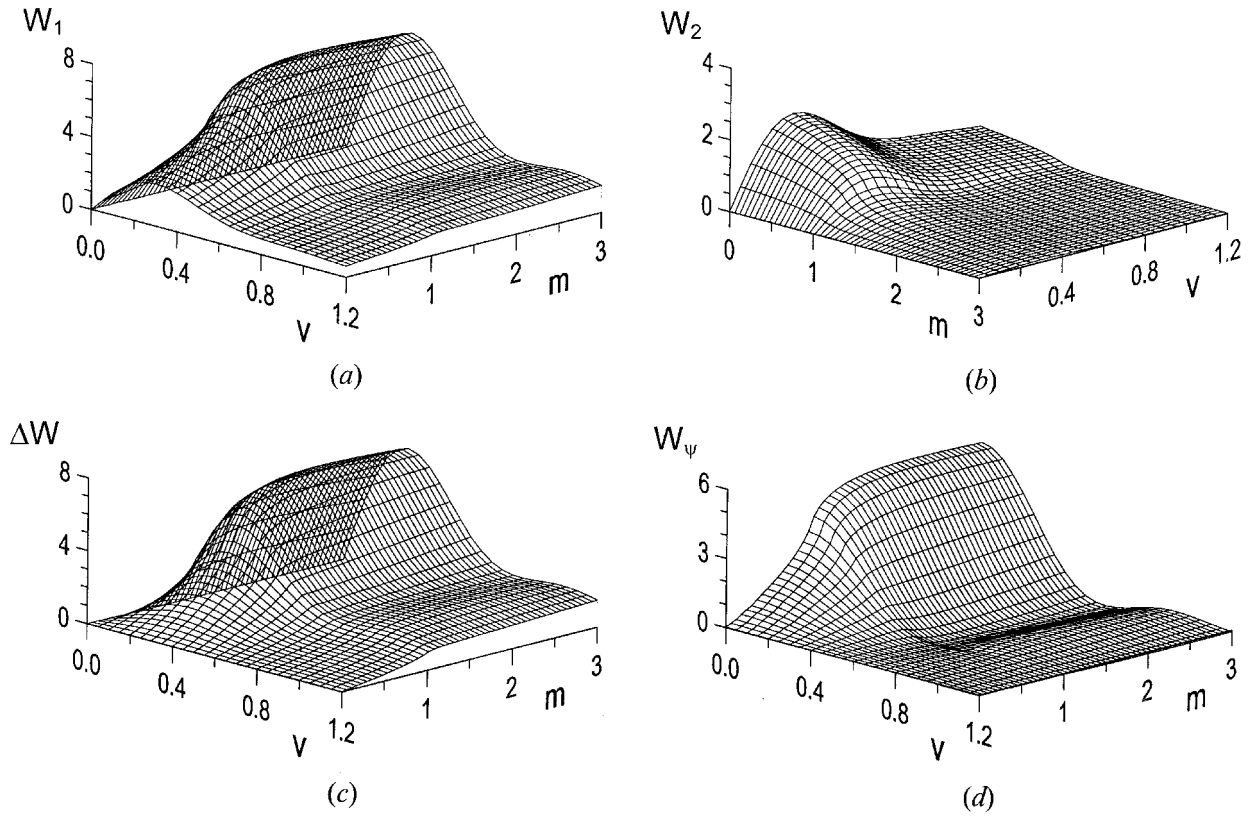

Figure 12. The characteristic surfaces for the reduced principal turbidities, $W_1(v_0, m)$ (*a*), $W_2(v_0, m)$ (*b*), parameter of dichriosm, $\Delta W(v_0, m) = W_1 - W_2$ (*c*), and reduced phase shift, $W_\psi(v_0, m)$ (*d*) of the uniaxially stretched monodisperse PDLC film at normal incidence, $\vartheta_F = \pi/2$; $n_o = n_m$.

steepness of the NCAP film's transmission curve decreases with the growth of v_{32}.

5.2.2. *The case of oblique incidence*

To represent the angular and field dependence of the polarized light transmission, we have calculated the *angular characteristic surfaces* for the principal reduced turbidities, $W_{1,2}(\vartheta_F, e_{32})$, and the reduced phase shift, $W_\psi(\vartheta_F, e_{32})$; the latter is entered by the relation $\psi \equiv (C_V d\Delta n/\lambda) W_\psi$. The relevant data are shown in figures 10 and 11 for the case of index matching, $n_o = n_m$.

As can be seen, the corresponding characteristic surfaces of PDLC and NCAP films have much in common. Nevertheless, there are certain differences concerned, first with the in-plane zero field ordering of bipolar droplets in the NCAP film, and second with the higher polydispersity of the NCAP film.

At zero field, $W_1(e=0)$ and $W_2(e=0)$ of the PDLC film do not depend on ϑ_F, while $W_\psi(e=0)=0$. This is an expected result in view of the spherical symmetry of the distribution of droplet directors in an unpowered dispersion of this morphology. On the contrary, for the NCAP film, $W_1(\vartheta_F, e_{32}=0)$ progressively decreases to zero, $W_2(\vartheta_F, e_{32}=0)$ remains nearly unchanged, and $W_\psi(e_{32}=0)\neq 0$ at large ϑ_F. Such a behaviour reflects the in-plane ordering of $\hat{\mathbf{N}}$ in the unpowered NCAP film: the component $\hat{\mathbf{e}}_\parallel$ of the incident wave becomes perpendicular to $\hat{\mathbf{N}}$ in all the droplets when $\vartheta_F \to 90°$, which reduces the scattering and phase shift of $\hat{\mathbf{e}}_\parallel$ as compared to $\hat{\mathbf{e}}_\perp$.

When e_{32} increases, the behaviour of the $W_1(e_{32})$ and $W_\psi(e_{32})$ substantially depends on ϑ_F. At small $v_{32} \leqslant 0{\cdot}3$, the region of decreasing $W_1(e_{32})$ regularly goes with ϑ_F into the region of increasing $W_1(e_{32})$, whereas $W_\psi(e_{32})$ is a monotonically increasing function at all $\vartheta_F > 0$. Alternatively, in all cases (except $n_o < n_m$) the W_2 is diminished with growing e_{32}, being practically independent of ϑ_F. This provides the increase in transparency of the film for $\perp$-polarized light at an arbitrary ϑ_F and, in combination with the behaviour of $W_1(e_{32}, v_{32})$, gives rise to a polarization effect on the natural light impinging at large incidence angle. When v_{32} is increased, the oscillations of $W_1(\vartheta_F)$ and $W_\psi(\vartheta_F)$ appear, being a manifestation of the diffraction effect. At high fields $e_{32} \gg 1$, the dependencies $W_1(\vartheta_F)$, $W_\psi(\vartheta_F)$ reproduce the shape of the corresponding curves $Q_1(\vartheta_F)$, $(P_1 - P_2)(\vartheta_F)$ shown in figure 7. For the NCAP film, the angular oscillations are smoothed due to a broad distribution of

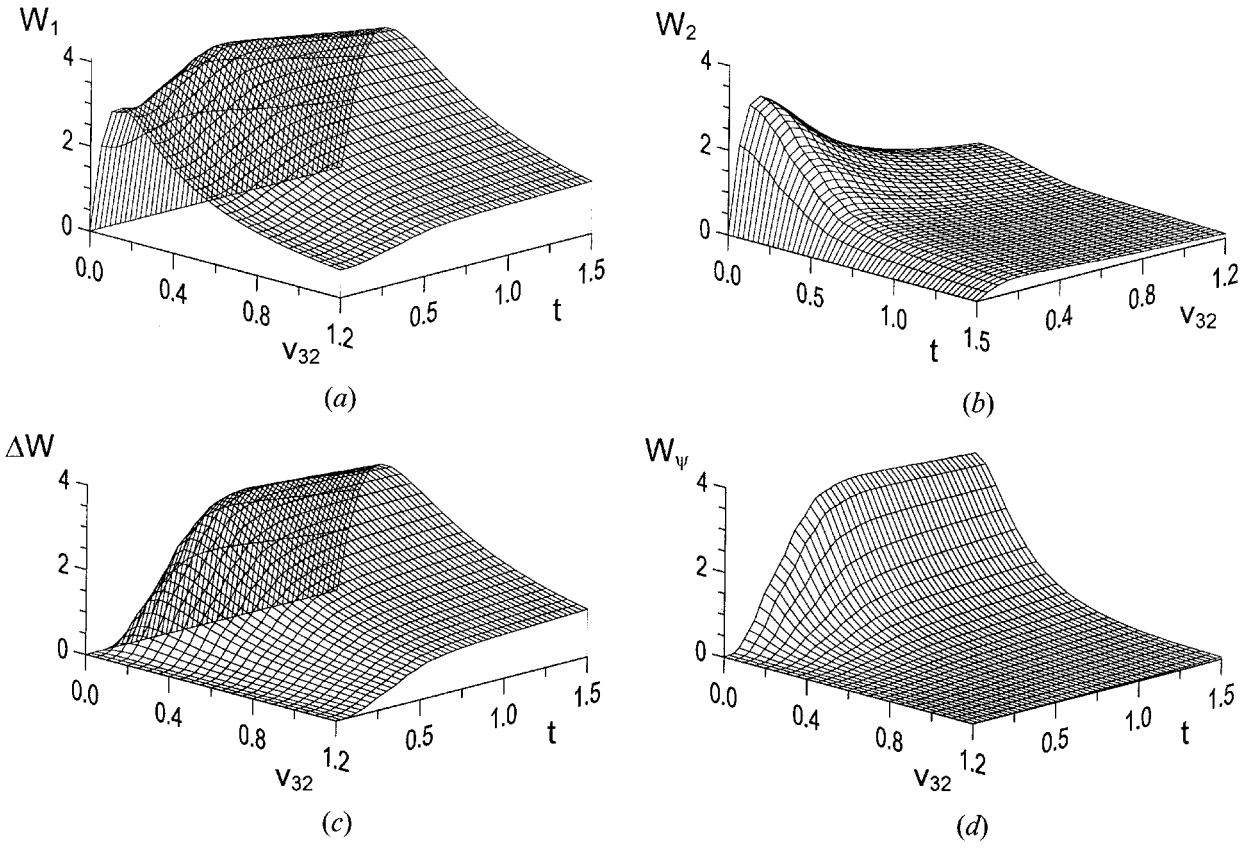

Figure 13. The characteristic surfaces for the reduced principal turbidities, $W_1(v_0, t)$ (*a*), $W_2(v_0, t)$ (*b*), parameter of dichriosm, $\Delta W(v_0, t) = W_1 - W_2$ (*c*), and reduced phase shift, $W_\psi(v_0, t)$ (*d*) of the uniaxially stretched polydisperse (SEM data) NCAP film at normal incidence, $\vartheta_F = \pi/2$; $n_o = n_m$.

droplet sizes. This case of the saturated film orientation has previously been analysed in detail by Whitehead *et al.* [3].

Additional calculations have shown that the surfaces $W_1(\vartheta_F, e_{32})$ and $W_2(\vartheta_F, e_{32})$ have only a weak dependence on the relative index mismatch $u = (n_o - n_m)/\Delta n$ if the latter varies in the range $-0{\cdot}1 < u < 0{\cdot}1$. By contrast, the $W_\psi(\vartheta_F, e_{32})$ surface is substantially modified: the phase shift can be negative (when $u < 0$), alternating ($u \approx 0$), or positive ($u > 0$).

It should be added that in the region $\vartheta_F < 30°$ and at $v_{32} < 0{\cdot}3$ our results for the phase shift are in agreement with the model of Basile *et al.* [13]. For larger v_{32}, we have observed considerable discrepancy since the model [13] takes no account of the diffraction phenomena.

5.3. *Stretching induced effects*

The reduced principal turbidities, W_1, W_2, the parameter of dichroism, $\Delta W = W_1 - W_2$, and the reduced phase shift, W_ψ, of the uniaxially stretched PDLC and NCAP films are shown as functions of parameters v_0, m and t in figures 12 and 13 for the case of normal incidence of light; v_0 denotes the value of v for the unstretched film. These characteristic surfaces are suitable for the optimization of PDLC polarizers [5–7].

The features common for both PDLC and NCAP films can be summarized as follows. Increase in the orientational ordering of the system leads to the regular increase in W_1, W_ψ and decrease in W_2. The shapes of $W_2(v_0, m)$ and $W_2(v_0, t)$ are therefore very similar to the shapes of surfaces $W(v_{32}, e_{32})$ shown in figures 8(*b*) and 9(*b*); this is because of the previously mentioned similarity between the stretching induced ordering and the field-controlled droplet reorientation. The above processes are responsible for the rise in the extinction anisotropy described by ΔW. At a given stretch parameter m or t, the position of the maximum of the dependence $\Delta W(v_0)$ is governed by $v_{0\max} = v_{0\max}^{(in)} p^{-\alpha}$, where $v_{0\max}^{(in)}$ corresponds to the maximum of $W(v_0)$ in the unstretched film, and the relationship between p, m, t is defined in §4. It is interesting to note that, for non-zero m and t, $\lim_{v_0 \to 0} W_\psi(v_0) \gg 0$ while $\lim_{v_0 \to \infty} W_\psi(v_0) = 0$; in other words, the film is more birefringent at small v. Mathematically, this is a result of the ratio $(P_1 - P_2)/v_0$ governing the behaviour of $W_\psi(v_0)$. A similar effect takes place in colloidal dispersions [29, 30].

It should be noted that we have ignored the birefringence of the stretched polymer matrix in our calculations. A separate analysis based on the available experimental data [6] has shown that the matrix birefringence is relatively small and has little impact on the characteristics of the transmitted light.

6. Conclusion

In conclusion, we have performed a systematic theoretical study of the stationary light transmission, linear dichroism and birefringence of nematic/polymer dispersions with an arbitrary degree of orientational ordering of the bipolar nematic droplets, and for an arbitrary angle of incidence of the probing light. Based on the single scattering approach and the anomalous diffraction approximation, we have analysed several important situations: PDLC and NCAP films in an external electric field, and PDLC and NCAP films under uniaxial mechanical deformation. The analysis has shown that the characteristic properties of the electro-optic and mechano-optic response of nematic/polymer dispersions can be described in terms of universal dimensionless functions which depend on the geometrical, material and structural parameters of the dispersion. The results obtained can be used for optimization of nematic/polymer composite films for projection displays, light shutters, and scattering polarizers, as well as for the solution of inverse problems in optics of polymer dispersed nematic liquid crystals.

References

[1] Doane, J. W., 1990, *Liquid Crystals: Applications and Uses*, edited by B. Bahadur (Singapore: World Scientific), Chap. 14, and references therein.

[2] Drzaic, P. S., 1995, *Liquid Crystal Dispersions*, (Singapore: World Scientific, Series on Liquid Crystals), and references therein.

[3] Whitehead, J. B., Zumer, S., and Doane, J. W., 1993, *J. appl. Phys.*, **73,** 1057.

[4] Wu, B.-G., West, J. L., and Doane, J. W., 1987, *J. appl. Phys.*, **62,** 3925.

[5] Zyryanov, V. Ya., Smorgon, S. L., and Shabanov, V. F., 1992, *Mol. Eng.*, **1,** 305.

[6] Aphonin, O. A., Panina, Yu. V., Pravdin, A. B., and Yakovlev, D. A., 1993, *Liq. Cryst.*, **15,** 395.

[7] Aphonin, O. A., 1995, *Liq. Cryst.*, **19,** 469.

[8] Bloisi, F., Ruocchio, C., Terrecuso, P., and Vicari, L., 1996, *Liq. Cryst.*, **20,** 377; 1996, *Opt. Lett.*, **21,** 95; 1996, *Phys. Rev. E*, **54,** 5242.

[9] Aphonin, O. A., and Nazvanov, V. F., 1997, *Mol. Cryst. liq. Cryst.* (in press).

[10] Van de Hulst, H. C., 1957, *Light Scattering by Small Particles* (New York: Wiley).

[11] Bohren, C. F., and Huffman, D. R., 1983, *Absorption and Scattering of Light by Small Particles* (New York: Wiley).

[12] Sansone, V. J., Khanarian, G., Leslie, T. M., Stiller, M., Altman, J., and Elizondo, P., 1990, *J. appl. Phys.*, **67,** 4253.

[13] Basile, F., Bloisi, F., Vicari, L., and Simoni, F., 1993, *Phys. Rev. E*, **48,** 432; 1994, *Mol. Cryst. liq. Cryst.*, **251,** 271.

[14] Vicari, L., 1997, *J. appl. Phys.*, **81,** 6612.

[15] Kelly, J., Wu, W., and Palffy-Muhoray, P., 1992, *Mol. Cryst. liq. Cryst.*, **223,** 251.

[16] Li, Z., Kelly, J. R., Palffy-Muhoray, P., and Rosenblatt, C., 1992, *Appl. Phys. Lett.*, **60,** 3132.

[17] Kelly, J., and Palffy-Muhoray, P., 1994, *Mol. Cryst. liq. Cryst.*, **243,** 11.

[18] Bloisi, F., Terreccuso, P., Vicari, L., and Simoni, F., 1995, *Mol. Cryst. liq. Cryst.*, **266,** 229; 1996, *Opt. Commun.*, **123,** 449.

[19] Drzaic, P. S., 1986, *J. appl. Phys.*, **60,** 2142.

[20] Aphonin, O. A., and Nazvanov, V. F., 1990, *Sov. Phys. Tech. Phys.*, **35,** 1168.

[21] Khlebtsov, N. G., 1984, *Zh. prikl. Spektrosk.*, **40,** 320.

[22] Zumer, S., Golemme, A., and Doane, J. W., 1989, *J. opt. Soc. Am. A*, **6,** 403.

[23] Kelly, J. R., and Wu, W., 1993, *Liq. Cryst.*, **14,** 1683.

[24] Naijzen, J. H. M., Boots, H. M. J., Paulissen, F. A. M. A., Van der Mark, M. B., and Cornelissen, H. J., 1997, *Liq. Cryst.*, **22,** 255.

[25] Zumer, S., 1988, *Phys. Rev. A*, **37,** 4006.

[26] Montgomery, G. P., Jr, West, J. L., and Tamura-Lis, W., 1991, *J. appl. Phys.*, **69,** 1605.

[27] Drzaic, P. S., and Gonzales, A. M., 1992, *Mol. Cryst. liq. Cryst.*, **222,** 11.

[28] Van de Hulst, H. C., 1980, *Multiple Light Scattering: Tables, Formulas, and Applications* (New York: Academic).

[29] Meeten, G. H., 1980, *J. Coll. Inter. Sci.*, **73,** 38.

[30] Khlebtsov, N. G., Melnikov, A. G., and Bogatyrev, V. A., 1991, *J. Coll. Inter. Sci.*, **146,** 463.

[31] Ondris-Crawford, R., Boyko, E. P., Wagner, B. G., Erdmann, J., Zumer, S., and Doane, J. W., 1991, *J. appl. Phys.*, **69,** 6380.

[32] Ding, J., and Yang, Y., 1992, *Jpn. J. appl. Phys.*, **31,** 2837.

[33] Yakovlev, D. A., and Aphonin, O. A., 1997, *Opt. Spectrosc.*, **82,** 78.

[34] Shifrin, K. S., 1983, *Introduction into Optics of the Ocean* (Leningrad: Gidrometeoizdat), in Russian.

[35] Wu, B.-G., Erdmann, J., and Doane, J. W., 1989, *Liq. Cryst.*, **5,** 1453.

[36] Drzaic, P. S., 1988, *Liq. Cryst.*, **3,** 1543.

[37] Havens, J. R., Leong, D. B., and Reimer, K. B., 1990, *Mol. Cryst. liq. Cryst.*, **178,** 89.

[38] Koval'chuk, A. V., Kurik, M. V., Lavrentovich, O. D., and Sergan, V. V., 1988, *Sov. Phys. JETP.*, **67,** 1069.

[39] Aphonin, O. A., 1996, *Mol. Cryst. liq. Cryst.*, **281,** 105; 1996, *Proc. SPIE*, **2731,** 168.

[40] Williams, R. D., 1986, *J. Phys. A*, **19,** 3211.

[41] Korn, G. A., and Korn, T. H., 1968, *Mathematical Handbook for Scientists and Engineers* (New York: McGraw-Hill), Chap. 6.

[42] Komura, S., Atkin, R. J., Stern, M. S., and Dunmur, D. A., 1995, *Mol. Cryst. liq. Cryst.*, **261,** 123.

[43] Drzaic, P. S., 1995, *Mol. Cryst. liq. Cryst.*, **261,** 383.

[44] Bosc, D., Trubert, S., Vinouze, B., and Guilbert, M., 1996, *Appl. Phys. Lett.*, **68,** 2489.

[45] Nomura, H., Suzuki, S., and Atarashi, Y., 1990, *Jpn. J. appl. Phys.*, **29,** 522.

[46] Wu, S.-T., Wu, C.-S., Warenghem, M., and Ismaili, M., 1993, *Opt. Eng.*, **32,** 1775.

[47] Speranskaya, T. A., and Tarutina, L. I., 1976, *Optical Properties of Polymers* (Leningrad: Khimiya), in Russian.